Chinese Chemical Letters 33 (2022) 3782–3786

Contents lists available at ScienceDirect

Chinese Chemical Letters

journal homepage: www.elsevier.com/locate/cclet

A multifunctional upconversion nanoparticles probe for Cu^{2+} sensing and pattern recognition of biothiols

Qian-Qian Wang[a,1], Rong Hu[a,1], Zheng-Qi Fang[a], Guoyue Shi[a], Shengqiang Zhang[b,*], Min Zhang[a,*]

[a] School of Chemistry and Molecular Engineering, Shanghai Key Laboratory for Urban Ecological Processes and Eco-Restoration, East China Normal University, Shanghai 200241, China
[b] Fujian Provincial Key Laboratory of Resources and Environment Monitoring & Sustainable Management and Utilization, College of resource and chemical engineering, Sanming University, Sanming 365004, China

ARTICLE INFO

Article history:
Received 24 August 2021
Revised 15 September 2021
Accepted 3 November 2021
Available online 10 November 2021

Keywords:
Upconversion nanomaterials
Polyacrylic acid
Copper ion
Pattern recognition sensor array
Biothiols

ABSTRACT

Lanthanide-doped upconversion nanoparticles (Ln-UCNPs) are a new type of nanomaterials with excellent fluorescence properties, which are well applied in fluorescent biosensing. Herein we developed a multifunctional probe based on the surface engineering of core-shell structure UCNPs with polyacrylic acid (PAA). The developed PAA/UCNPs probe could be highly selective to detect and respond to Cu^{2+} at different pH. Cu^{2+} could easily combine with the carboxylate anion of PAA to quench the fluorescence of UCNPs. Therefore, we creatively proposed a fluorescent array sensor (PAA/UCNPs-Cu^{2+}), in which the same material acted as the sensing element by coupled with pH regulation for pattern recognition of 5 thiols. It could also easily identify the chiral enantiomer of cystine (L-Cys-and D-Cys), and distinguish their mixed samples with different concentrations, and more importantly, it could be combined with urine samples to detect actual level of homocysteine (Hcys) to provide a new solution for judging whether the human body suffers from homocystinuria.

Metal ions are widely regarded as important chemical substances involved in the metabolism of living body. Copper ion (Cu^{2+}) is essential for human life and health [1,2], playing a very important role in the process of peptide amidation, neurotransmitter synthesis, and cell respiration [3]. The normal concentration of Cu^{2+} in human blood is 100–150 μg/dL (15.7–23.6 μmol/L) [4], however, it is harmful to the body when higher than normal concentration. The destruction of Cu^{2+} homeostasis will further damage the body and cause a variety of neurodegenerative diseases, such as Alzheimer's disease and Wilson's disease [1,5-8]. With the rapid development of industrial application technology, a large amount of Cu^{2+} is used in the environment, metallurgy, medicine, information and other fields, resulting in excessive copper emissions and causing serious damage to the environment and life systems. The U.S. Environmental Protection Agency (EPA) expressly stipulates that the concentration of Cu^{2+} in daily drinking water cannot exceed 20 μmol/L [9]. Therefore, the analysis of Cu^{2+} has extraordinary significance for both human health and ecological protection. The current methods detecting Cu^{2+} mainly include electrochemical method [10], electrochemiluminescence method [11], atomic absorption spectrometry (AAS) [12], inductively coupled plasma-atomic emission spectrometry (ICP-AES) [13] and fluorescence method [14,15]. Fluorescence method has unique advantages such as fast, simple, good selectivity, and can realize *in-situ* online monitoring, and has attracted more and more attention in production and life.

Thiols, a kind of important biomarker which has a strong interaction with Cu^{2+}, also act as an important research object in life sciences and other fields. The disordered level of thiols in biofluids usually has relation to cardiovascular and cerebrovascular diseases [16], neurodegenerative diseases [17] and certain cancers [18]. For example, the normal level of homocysteine (Hcys) in urine is 5–15 μmol/L, while in the urine of patients with homocystinuria is usually higher than 50 μmol/L [19]. Homocystinuria is a disease caused by the lack of cystathionine beta synthase [20], accompanied with mental retardation, developmental delay and abnormal cardiovascular system. There are many kinds of thiols in biological fluids, such as glutathione (GSH), cysteine (Cys), homocysteine (Hcys), *N*-acetylcysteine (NAC). Different types of thiols are

* Corresponding authors.
E-mail addresses: shengqiang.zhang@vip.163.com (S. Zhang), mzhang@chem.ecnu.edu.cn (M. Zhang).
[1] These authors contributed equally to this work.

https://doi.org/10.1016/j.cclet.2021.11.012
1001-8417/

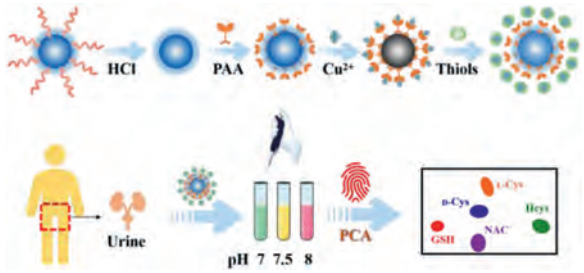

Scheme 1. Schematic illustration of the fluorescence probe based on PAA-modified UCNPs for Cu^{2+} and thiols detection.

very similar in chemical structure and properties. Therefore, distinguishing multiple thiols is the main problem to be solved urgently. The traditional sensor recognition strategy is based on the "lock and key" sensing mode, that is, one probe can only specifically recognize one target, which is not conducive to the identification and detection of multiple target substances or mixed samples. However, the "chemical tongue" sensor arrays based on pattern recognition have emerged in recent years could recognize a variety of analytes at high-throughput [21–24].Traditional fluorescence materials (quantum dots, organic dyes, *etc.*) mostly exhibit emission based on Stokes's shift, and have inevitable shortcomings such as photobleaching, wide emission band and biological toxicity [25]. Lanthanide-doped upconversion nanoparticles (Ln-UCNPs) are a new type of nanomaterials with excellent fluorescence properties that can convert low-energy near-infrared light into high-energy ultraviolet or visible light [26]. They have many inherent advantages, such as narrow emission band, strong penetrating ability, low biological toxicity and weak autofluorescence. Furthermore, they have broad development and application prospects in the fields of biosensing and optical sensor manufacturing [22,27-30]. UCNPs-based fluorescence analysis has been extensively developed for the specific analyte. However, there are few reports on UCNPs-based multifunctional assays to discriminate multiple targets.

Herein, by surface engineering of ligand-free UCNPs with polyacrylic acid (PAA), a PAA/UCNPs probe was constructed in PBS buffer to rapidly and sensitively detect Cu^{2+}. Furthermore, a novel sensor array was developed based on a pH regulation strategy, realizing the pattern recognition of thiols (Scheme 1). Firstly, oleic acid (OA)-capped $NaYF_4$: 20%Yb, 0.5%Tm@$NaGdF_4$ (OA-UCNPs) with core-shell structure was synthesized by solvothermal method [31], and then the OA ligand on the surface of OA-UCNPs was removed by acid treatment to obtain ligand-free UCNPs with good water dispersibility [22,32]. Then, ligand-free UCNPs can be readily modified with PAA. Since copper carboxylate complexes could be formed due to the complexation of Cu^{2+} and PAA, the fluorescence of PAA/UCNPs will be quenched ("turned off") after the addition of Cu^{2+} in the buffer system. And the fluorescence intensity of the PAA/UCNPs probe gradually decreased with the increase of Cu^{2+}, thus realizing the detection of Cu^{2+} under the excitation of near-infrared light with a low-cost, high-sensitivity strategy. More importantly, due to the differential fluorescence response of PAA/UCNPs probe to Cu^{2+} under different pH conditions, an innovative "chemical tongue" fluorescence sensor array was developed, that is, PAA/UCNPs-Cu^{2+} under buffer systems with three different pH values was composed as our proposed sensor array. Inspired by the easy and somewhat different coordination of Cu^{2+} with sulfhydryl groups, a data matrix composed of intricate responses of various thiols to the sensor array was obtained. Then, various thiols could be clearly recognized and the chiral enantiomers of Cys-could be well distinguished by principal component analysis (PCA). Our presented PAA/UCNPs sensor array was further applied to non-invasively analyze Hcys in urine, providing a new solution

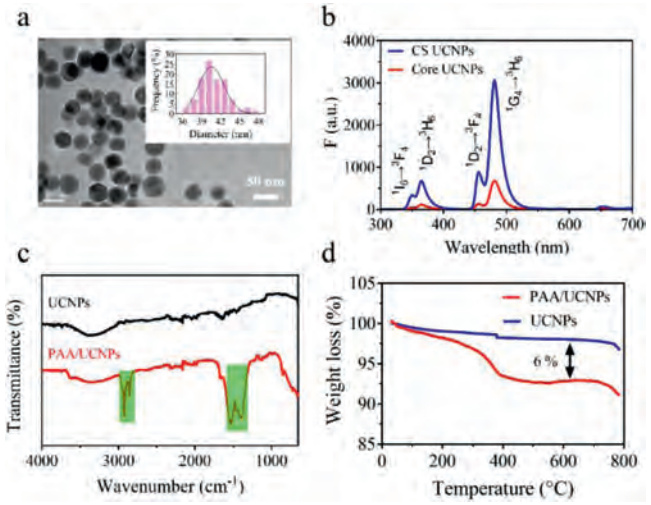

Fig. 1. (a) TEM image of the core-shell UCNPs $NaYF_4$: 20%Yb, 0.5%Tm@$NaGdF_4$ and the corresponding particle size distribution. (b) Upconversion fluorescence spectra of core UCNPs and core-shell UCNPs under the same conditions. (c) FTIR spectrum and (d) TG analyses of the UCNPs and PAA/UCNPs (UCNPs refer to ligand-free UCNPs).

for checking whether the human body suffers from homocystinuria.

OA-UCNPs with core-shell structure were prepared by solvothermal method, and the morphology of the obtained UCNPs was characterized by TEM (Fig. 1a). The results showed that UCNPs present a regular hexagonal core-shell structure and a uniform particle size distribution of 40.8 ± 5.3 nm. In addition, the particle size distribution of core UCNPs was uniformly 29.5 ± 3.7 nm (Fig. S1 in Supporting information). Therefore, the inert shell thickness of core-shell UCNPs was about 5 nm. Next, the prepared UCNPs were dispersed in cyclohexane and excited by a near-infrared 980 nm laser to characterize the fluorescence feature of UCNPs (Fig. 1b). Due to the $^1I_6 \rightarrow {}^3F_4$, $^1D_2 \rightarrow {}^3H_6$, $^1D_2 \rightarrow {}^3F_4$ and $^1G_4 \rightarrow {}^3H_6$ transitions of the activator Tm^{3+}, there were obvious upconversion fluorescence emission peaks at 350 nm, 368 nm, 455 nm and 484 nm. The main emission peak at 484 nm had the strongest fluorescence intensity, which was used in our subsequent analysis and testing experiments. It was important to note that the fluorescence emission intensity of core-shell UCNPs was about 4.46 times stronger than that of core UCNPs. It's because that the inert shell not only served as a spacer matrix to isolate the activator and ligands or solvent molecules and other quenching substances, but also could modify the lattice defects on the surface of the core [33]. The significant enhancement of the fluorescence intensity of core-shell UCNPs could greatly improve the sensitivity of the probe/sensor made with it, reduce the amount of material, and be excited by a lower excitation light to reduce the thermal effect of the reaction system.

After removing the oleic acid (OA) ligand, water-dispersible ligand-free UCNPs were engineered with PAA to obtain a hybrid of PAA/UCNPs. Then we carried out various characterizations on ligand-free UCNPs and PAA/UCNPs respectively. First, FT-IR spectroscopy proved the successful construction of PAA/UCNPs (Fig. 1c). It could be clearly seen that there were characteristic peaks at 1540 cm^{-1} and 1410 cm^{-1}, which were attributed to the asymmetric stretching vibration of the carbonyl group and the carbon-oxygen single bond of the PAA functional group, respectively [34]. At the same time, we noticed that the characteristic peaks (1420, 1560, 2850, 2920 cm^{-1}) attributable to OA on UCNPs disappeared, which proved that OA had been successfully removed and they were ligand-free UCNPs. In addition, the zeta potential of UCNPs

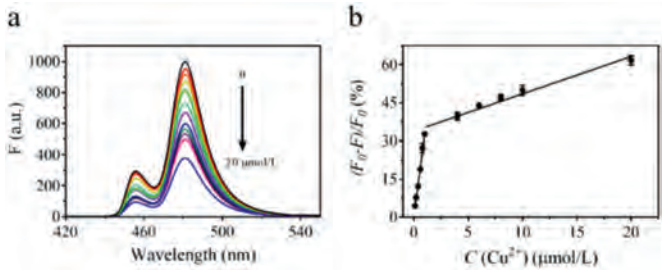

Fig. 2. (a) The upconversion fluorescence spectra of PAA/UCNPs probe incubated with various concentration of Cu^{2+} (0–20 μmol/L). (b) The plot of fluorescence intensity quenching efficiency $(F - F_0)/F_0$ (%) *versus* the concentration of Cu^{2+} (0–20 μmol/L).

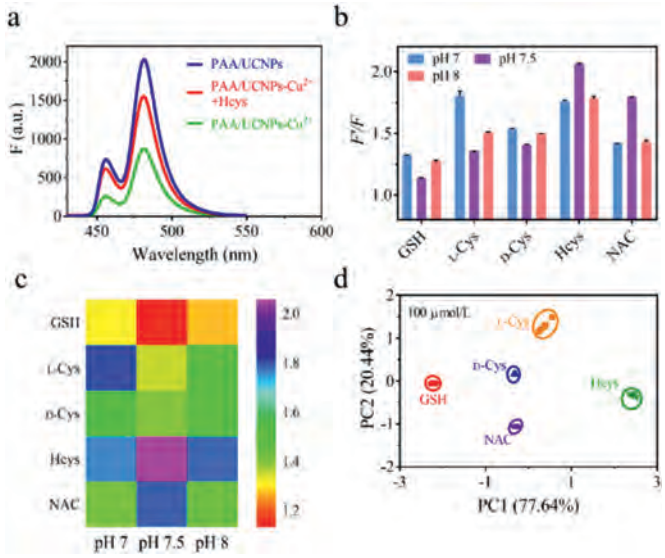

Fig. 3. (a) Upconversion fluorescence spectra of PAA/UCNPs, PAA/UCNPs-Cu^{2+} and PAA/UCNPs-Cu^{2+}+Hcys. (b) Upconversion fluorescence patterns of the pH-regulated PAA/UCNPs-Cu^{2+} sensor array toward GSH, L-Cys, D-Cys, Hcys, and NAC. (c) Heat map and (d) canonical score plot derived from upconversion fluorescence patterns of the presented sensor array toward thiols indicated, where F and F' represent the upconversion fluorescence intensity at 484 nm of the pH regulated PAA/UCNPs-Cu^{2+} sensor array before and after the addition of thiols, respectively.

was measured to be +27.5 mV, which made the ligand-free UCNPs present a stable colloidal state in the aqueous dispersion. And the positive potential of UCNPs was mainly due to the fact that there were many positive rare earth ions on the surface of bare UCNPs. But PAA/UCNPs had a very negative zeta potential of −28.6 mV, which proved that UCNPs were functionalized by PAA (Fig. S2 in Supporting information). Furthermore, we quantified the percentage of PAA in the PAA/UCNPs by TG analysis to be about 6 wt% (Fig. 1d). All the above facts displayed that the PAA/UCNPs were successfully prepared and could be well applied for further experimental investigation.

In the presence of Cu^{2+}, the carboxylate anion of PAA/UCNPs could combine with it to form a copper carboxylate complex to quench the fluorescence of UCNPs [34]. Based on this, PAA/UCNPs were qualified for the analysis of Cu^{2+}. The response of the upconversion fluorescence intensity of PAA/UCNPs was recorded by adding various concentrations of Cu^{2+}. First of all, we optimized the experimental conditions. It cannot be ignored that pH could affect the quenching effect of Cu^{2+} on PAA/UCNPs. As shown in Fig. S3a (Supporting information), the changes of the fluorescence intensity of PAA/UCNPs before and after the addition of Cu^{2+} were measured under different pH values. And we could see that the degree of fluorescence quenching was greatest at pH 8.0. Therefore, we chose PBS buffer at pH 8.0 for subsequent reactions. The degree of fluorescence quenching was mainly measured by "$(F_0 - F)/F_0$ (%)", where F_0 and F represented the upconversion fluorescence intensity before and after the addition of Cu^{2+} respectively. In addition, we explored the relationship between the degree of quenching and reaction time, found that the response of PAA/UCNPs to Cu^{2+} was rapid. The time to reach the quenching plateau value was evaluated to 15 min (Fig. S3b in Supporting information), which was much shorter than 60-minute response time of UCNPs for Cu^{2+} sensing previously reported in the literature [22]. These results proved that a liable and convenient Cu^{2+} probe had been successfully constructed.

As shown in Fig. 2a, the upconversion fluorescence intensity of PAA/UCNPs showed a gradual decrease as the concentration of Cu^{2+} increases. The fluorescence quenching efficiency was linearly correlated with the concentration of Cu^{2+} when it is in the range of 0.1–1 μmol/L and 1–20 μmol/L, respectively (Fig. 2b). The two regression equations were described as $Y = 31.84X + 0.706$ ($R^2 = 0.986$) and $Y = 1.475X + 33.73$ ($R^2 = 0.950$) respectively. LOD was calculated to be 0.019 μmol/L ($3\delta/S$). The above results indicated that PAA/UCNPs probe had the potential to detect low concentrations of Cu^{2+}, meeting the requirements of EPA standard (≤ 20 μmol/L) [24]. The selectivity of PAA/UCNPs probe was also explored. we selected 11 metal ions (Co^{2+}, Pb^{2+}, Ni^{+}, Zn^{2+}, Ca^{2+}, Cr^{3+}, Li^{+}, Al^{3+}, Mn^{2+}, Mg^{2+}, Fe^{3+}) with a final concentration of 50 μmol/L for interference test. As shown in Fig. S4 (Supporting information), the influence of other metal ions on our probe was almost negligible, which proved that this probe had good selectivity toward Cu^{2+} sensing. Based on previous studies [35], the most likely quenching mechanism at low metal ion concentrations is dynamic quenching, which is the result of collisions around UCNPs and Cu^{2+}. Static quenching, which forms complex between Cu^{2+} and UCNPs at ground state, occurs at higher concentrations.

In order to evaluate the potential application value of PAA/UCNPs, it is necessary to further study the feasibility of detecting Cu^{2+} in biofluids. For instance, the level of Cu^{2+} in the urine of patients with Wilson's disease is abnormal, and urinary copper is a key indicator of the disease [36]. Also, it is very important to accurately determine the concentration of Cu^{2+} in urine. Therefore, we prepared artificial urine and artificial saliva. And a series of biofluid samples containing various concentrations of Cu^{2+} were added to PAA/UCNPs to determine the concentration of Cu^{2+}. The resultant test had the recovery between 97% and 108% (Table S2 in Supporting information), suggesting the good applicability of the proposed method to real analysis of Cu^{2+} in biological samples. Furthermore, the accuracy of our method was verified by the traditional standard ICP-AES method. And the relative standard deviation (RSD, $n = 3$) of the test results was all within 5%. Real sample experiments with urine and saliva obtained non-invasively showed that our proposed method had great promise in practical application.

Inspired by the easy coordination of Cu^{2+} with sulfhydryl groups, we believed that thiols could recovery the fluorescence of PAA/UCNPs quenched by Cu^{2+}. That is, when PAA/UCNPs were combined with Cu^{2+}, a PAA/UCNPs-Cu^{2+} sensor could be formed for the further analysis of thiols. As a proof-of-concept, the common thiol, Hcys, was picked to be added to PAA/UCNPs-Cu^{2+}, and the fluorescence spectrum was shown in Fig. 3a. Obviously, the fluorescence of PAA/UCNPs quenched by Cu^{2+} could be restored by Hcys. This is mainly because the binding capacity of Cu^{2+} to the thiol was greater than its binding ability to PAA. As shown in Fig. S5 (Supporting information), the PAA/UCNP luminescence is stable in the pH range of 6.5–8.5 on the whole. Moreover, in Fig. S3 (Supporting information), the fluorescence response of PAA/UCNPs probe to Cu^{2+} was different under distinct pH conditions. Thus, we proposed that PAA/UCNPs-Cu^{2+} at three different pH could be

picked as three sensing elements, and a "chemical tongue" fluorescence sensor array based on pH regulation for pattern recognition of thiols could be developed. 3 PBS buffers with appropriate pH (7.0, 7.5, 8.0) were prepared as the sensor array and 5 thiols (L-Cys, D-Cys, GSH, Hcys, NAC) with a final concentration of 100 μmol/L were added in buffer as targets. *F'/F* of the upconversion fluorescence intensity of PAA/UCNPs-Cu^{2+} before and after adding thiols was calculated to verify the feasibility of this sensor array for thiol analysis. *F'* and *F* represented the fluorescence intensity at 484 nm of the pH-regulated PAA/UCNPs-Cu^{2+} sensor array with and without the addition of thiol respectively. It could be seen from the fluorescence response histogram (Fig. 3b) and the heat map (Fig. 3c) that different thiols had distinct responses to the three sensing elements. The fluorescence data matrix "3 PAA/UCNPs-Cu^{2+} sensing elements × 5 thiols × 5 sets of repetitions" was analyzed and processed using the principal component analysis method. Principal component analysis (PCA) was performed to cut down the dimension of the data and concentrate the most prominent features which can represent the data matrices. And the typical factors are derived from data processing by SPSS 25.0 software (IBM). In this way, the typical factors of pattern recognition responses were obtained, and the two most important factors (PC1 and PC2) were exploited to draw the canonical score plot (Fig. 3d). The results displayed that 5 thiols were 5 independent clusters, which proved that these 5 thiols were independent of each other and could be distinguished by our sensor array. And it was worth emphasizing that the two enantiomers (L-Cys-and D-Cys) were also independent of each other in the PCA diagram, confirming the potential of the developed pH-regulated PAA/UCNPs-Cu^{2+} sensor array in distinguishing chiral enantiomers.

After successfully distinguishing the five thiols, L-Cys-and Hcys were utilized for quantitative analysis to further determine the analytical performances of our sensor array. Various concentrations of L-Cys-and Hcys were added to pH-regulated PAA/UCNPs-Cu^{2+} sensor array to obtain upconversion fluorescence intensity data. Upconversion fluorescence patterns and heat map of L-Cys and Hcys were shown in Figs. S6 and S7 (Supporting information), where *F'/F* represented the degree of fluorescence recovery of PAA/UCNPs-Cu^{2+} sensor array in the presence of thiol. After processing the data matrix with the PCA method, we could see that the clusters corresponding to various concentrations were regularly arranged in accordance with concentration (Figs. 4a and c). Since PC2 in the PCA plots was smaller than 3%, it was acceptable to employ PC1 to correlate the concentrations of L-Cys and Hcys. As shown in Fig. 4b, PC1 was effectively correlated with the concentrations of L-Cys at 1–100 μmol/L, and the linear range was 1–40 μmol/L. Meanwhile, there was a certain relationship between PC1 and the concentration of Hcys at 0.5–100 μmol/L, and a linear correlation at 0.5–20 μmol/L (Fig. 4d). These results indicate that our sensor array can distinguish different concentrations of thiols and this method can be applied for differentiation of biothiols with unknown concentrations according to above linear relationship.

Moreover, the constructed pH-regulated PAA/UCNPs-Cu^{2+} sensor array could also realize the analysis of mixed thiol samples, showing excellent performance in a complex environment. As shown in Fig. 5a, the PAA/UCNPs-Cu^{2+} sensor array was effective in the discrimination of 80 μmol/L Hcys and GSH mixture with Hcys/GSH molar ratios of 0/80, 10/70, 20/60, 40/40, 60/20, 70/10, 80/0. The corresponding upconversion fluorescence patterns and heat map were shown in Fig. S8 (Supporting information). The difference in the fluorescence response of the mixed samples was mainly due to the difference in the affinity of various types of thiols for Cu^{2+}, which led to the differential inhibition of the fluorescence of PAA/UCNPs by Cu^{2+}.

Chiral phenomena are ubiquitous in the colorful world we live in and play an important role in the fields of life sciences and

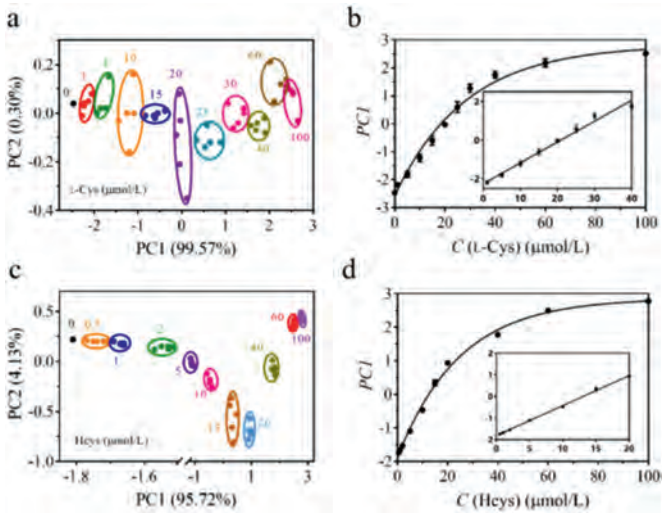

Fig. 4. (a) Canonical score plot derived from upconversion fluorescence patterns of the presented sensor array toward various concentrations of L-Cys-and (b) the plot of PC1 *vs.* the concentration of L-Cys. (c) Canonical score plot derived from upconversion fluorescence patterns of the presented sensor array toward various concentrations of Hcys and (d) the plot of PC1 *vs.* the concentration of Hcys.

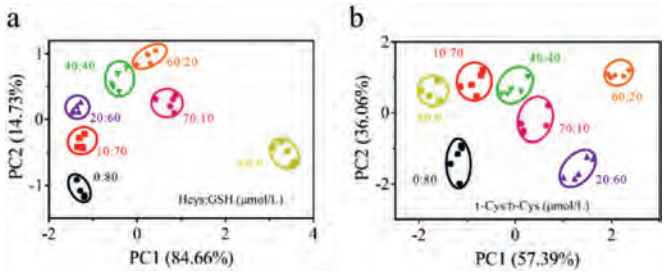

Fig. 5. Canonical score plot of the presented sensor array toward the mixture of (a) Hcys and GSH and (b) L-Cys-and D-Cys-with various molar rations.

medicinal chemistry. The identification of chiral molecules has always been the focus of scientific research. Hence, two enantiomers of Cys (L-Cys and D-Cys) were chosen to confirm the performances of our sensor array for chiral recognition (Fig. S9 in Supporting information). As shown in Fig. 5b, different molar ratios of L-Cys and D-Cys mixtures (0/80, 10/70, 20/60, 40/40, 60/20, 70/10, 80/0, μmol/L) could be fully differentiated from each other in the PCA plot, highlighting the capacity of our sensor array for chiral recognition. Compared with traditional chromatographic methods, our proposed sensor array for chiral recognition was cost-effective and easy to use.

In addition to analyzing thiols in the buffer system, the sensor array was further applied to biofluids to monitor human health. It is well known that Hcys plays an important role in homocystinuria, a disease caused by a lack of cystathionine beta synthase, which is characterized by increased excretion of Hcys in urine. Generally speaking, the normal level of Hcys is about 5–15 μmol/L, while the urine of homocystinuria patients would excrete higher levels of Hcys (>50 μmol/L). To further verify the feasibility of the proposed sensor array in non-invasive detection of thiols for health monitoring, the sensor array was applied to test samples of artificial urine added with Hcys (Fig. 6). The PCA plot and barcode-like heat map could provide flush references regarding the normal or abnormal level of Hcys for homocystinuria monitoring (*i.e.*, healthy or suffering).

In this work, highly sensitive and rapid detection of Cu^{2+} with a detection time of 15 min and a low detection limit of 0.019 μmol/L was accomplished by PAA/UCNPs probe. Meanwhile, a "chemical

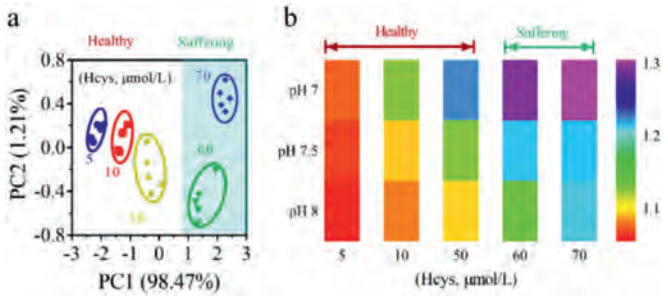

Fig. 6. (a) Canonical score plot and (b) barcode-like heat map for PAA/UCNPs-Cu^{2+} sensor array based on pH regulation for pattern recognition of Hcys in urine.

tongue" fluorescence sensor array was further constructed based on pH-regulated PAA/UCNPs-Cu^{2+}. Only one material was used as the sensing element, and the five thiols could be identified by changing the pH of the buffer system. Significantly, the prepared sensor array was able to discriminate mixtures of thiols as well as recognition of chiral enantiomeric mixtures of Cys, leading to a variety of multifunctional and powerful biosensing applications. Moreover, the application in real samples indicated that it could be a brilliant method for the development of non-invasive health monitoring. In short, due to its attractive advantages, the fluorescence sensing system developed by PAA-modified UCNPs has extraordinary guiding significance for the development of single-component sensor arrays, and has shown great significance in environmental monitoring, disease diagnosis or specific biological purposes.

Declaration of competing interest

The authors declare no conflict of interest.

Acknowledgments

This work was supported by the National Natural Science Foundation of China (No. 21775044), the Shanghai Science and Technology Committee (Nos. 19ZR1473300 and 18DZ1112700), and the Fundamental Research Funds for the Central Universities.

Supplementary materials

Supplementary material associated with this article can be found, in the online version, at doi:10.1016/j.cclet.2021.11.012.

References

[1] S. Sarkar, M. Chatti, V. Adusumalli, et al., ACS Appl. Mater. Interfaces 7 (2015) 25702–25708.
[2] A. Sikdar, S. Roy, R. Mahto, et al., ChemistrySelect 3 (2018) 13103–13109.
[3] V. Desai, S.G. Kaler, Am. J. Clin. Nutr. 88 (2008) 855S–858S.
[4] A. Helal, M. Harun, C. Cho, et al., Tetrahedron 67 (2011) 2794–2802.
[5] G. Georgopoulos, A. Roy, M.J. Yono, et al., J. Toxicol. Environ. Health Part B 4 (2001) 341–394.
[6] K.J. Barnham, C.L. Masters, A.I. BushK, Nat. Rev. Drug Discovery 3 (2004) 205–214.
[7] S. Mare, S. Penugonda, S.M. Robinson, et al., Peptides 28 (2007) 1424–1432.
[8] J.C. Lee, H.B. Gray, J.R. Winkler, J. Am. Chem. Soc 130 (2008) 6898–6899.
[9] J.L. Yao, K. Zhang, H.J. Zhu, et al., Anal. Chem. 85 (2013) 6461–6468.
[10] A.C. Liu, D.C. Chen, C.C. Lin, et al., Anal. Chem. 71 (1999) 1549–1552.
[11] L. Zhang, S. Li, S. Dong, Electrochem. Commun. 10 (2008) 1452–1454.
[12] T.W. Lin, S.D. Huang, Anal. Chem. 73 (2001) 4319–4325.
[13] Y. Liu, P. Liang, L. Guo, Talanta 68 (2005) 25–30.
[14] Q.X. Wang, S.F. Xue, Z.H. Chen, et al., Biosens. Bioelectron. 94 (2017) 388–393.
[15] J.Q. Chen, S.F. Xue, Z.H. Chen, et al., Biosens. Bioelectron. 100 (2018) 526–532.
[16] U. Singh, I. Jialal, Pathophysiology 13 (2006) 129–142.
[17] K. Sas, H. Robotka, J. Toldi, et al., Neurol. Sci. 257 (2007) 221–239.
[18] V.L. Kinnula, J.D. Crapo, Free Radicals Biol. Med. 36 (2004) 718–744.
[19] X.Y. Han, Z.H. Chen, J.Z. Zeng, et al., ACS Appl. Mater. Interfaces 10 (2018) 31725–31734.
[20] P.W.F. Wilson, JAMA 288 (2002) 2042–2043.
[21] Z.Y. Lin, Z.B. Qu, Z.H. Chen, et al., Anal. Chem. 91 (2019) 11170–11177.
[22] Q. Yan, X.Y. Ding, Z.H. Chen, et al., Anal. Chem. 90 (2018) 10536–10542.
[23] M.K. Nakhleh, H. Amal, R. Jeries, et al., ACS Nano 11 (2017) 112–125.
[24] H. Jin, Y.S. Abu-Raya, H. Haick, Adv. Healthcare Mater. 6 (2017) 1700024–1700043.
[25] C. Wang, X. Li, F. Zhang, Analyst 141 (2016) 3601–3620.
[26] G. Chen, H. Qiu, P.N. Prasad, et al., Chem. Rev. 114 (2014) 5161–5214.
[27] Z. Qiu, J. Shu, D. Tang, Anal. Chem. 90 (2018) 12214–12220.
[28] L. Lyu, H. Cheong, X. Ai, et al., NPG Asia Mater. 10 (2018) 685–702.
[29] Q. Yan, Z.H. Chen, S.F. Xue, et al., Sens. Actuators B 268 (2018) 108–114.
[30] Q. Li, X. Li, L. Zhang, et al., Nanoscale 10 (2018) 12356–12363.
[31] S. Han, A. Samanta, X. Xie, et al., Adv. Mater. 29 (2017) 1700244–1700250.
[32] L. Zhou, Y. Fan, R. Wang, et al., Angew. Chem. Int. Ed. 57 (2018) 12824–12829.
[33] S. Lahtinen, A. Lyytikäinen, N. Sirkka, et al., Microchim. Acta 185 (2018) 220–227.
[34] Y. Wang, Nanoscale 11 (2019) 10852–10858.
[35] S.M. Saleh, R. Ali, O.S. Wolfbeis, Chem. Eur. J. 17 (2011) 14611–14617.
[36] S. Su, Z. Mo, G. Tan, et al., Front. Chem. 8 (2021) 619764–619776.